23rd ABCM International Congress of Mechanical Engineering
December 6-11, 2015, Rio de Janeiro, RJ, Brazil

APPLYING DIFFERENT HEAT FLUX INTENSITIES TO ESTIMATE TEMPERATURE-DEPENDENT THERMAL PROPERTIES OF METALS

Luís Felipe dos Santos Carollo, felipecarollo@yahoo.com.br
Ana Lúcia Fernandes de Lima e Silva, alfsilva@unifei.edu.br
Sandro Metrevelle Marcondes de Lima e Silva, metrevel@unifei.edu.br
Federal University of Itajubá – UNIFEI, Institute of Mechanical Engineering – IEM, Heat Transfer Laboratory – LabTC, BPS Av., 1303, Pinheirinho District, Zip code 37500-903, Box Postal 50, Itajubá, MG, Brazil.

Abstract. *This work presents a method for the simultaneous estimation of temperature-dependent thermal conductivity, λ, and volumetric heat capacity, ρc_p, in samples of AISI 1045 steel. In this method, these properties are estimated simultaneously using the same experiment. Due to the initial temperature variation, the assembly is placed inside an oven. This model uses a constant heat flux on the upper surface of the sample and insulation condition on the bottom surface and the temperature is measured on the bottom surface by using type T thermocouple. Thus, the estimation of the properties is based on the analysis of the sensitivity coefficients. Based on this analysis, two different heat flux intensities are used. To estimate these properties, an objective function is minimized by applying the optimization technique BFGS. This function is defined by the square difference between the numerical and experimental temperatures plus the square of the systematic error caused by the thermal contact resistance. The numerical temperature is obtained by the solution of the proposed thermal model by using the Finite Difference method with an implicit formulation. Besides, uncertainty analyses are performed in order to ensure the quality of the obtained results. The estimated properties and the uncertainty are in good agreement with literature.*

Keywords: *thermal properties of metals, heat conduction, optimization, sensitivity coefficients, uncertainty.*

1. INTRODUCTION

Nowadays, due to globalization, more and more new techniques are required to quickly, reliably and accurately determine temperature-dependent thermophysical properties of materials. Another important aspect is the economic issue, because the lower the cost to determine the parameters, ensuring reliability, the greater the chance to compete in the national and international markets. The technique proposed in this paper can be used, for example, to correctly choose, under the point of view of thermal properties, the materials to be used in the manufacture of a heat exchanger. This choice is made by taking into account the values of thermophysical properties, which should be ideal to yield a saving that is directly linked to energy and environmental issues, widely discussed in the current global circumstances. Another example can be a machining process where great part of the heat generated by friction between the workpiece and the cutting tool must be transferred to the tool holder, as tool wear is directly linked to temperature increase. Thus, the right tool for the process can be chosen with the knowledge of its thermal conductivity which determines the range of the working temperature of the material. From these needs, researchers have developed many techniques which are being improved continuously (Santos *et al.*, 2014 and Brito *et al*., 2015).

There are several techniques to determine the thermophysical properties of diverse materials (Jannot *et al.*, 2009, Xamán *et al.*, 2009 and Thomas *et al.*, 2010). These techniques may determine these properties separately or isolatedly, and most of these estimations occur rapidly, safely and precisely. However, these techniques do not allow the temperature-dependent estimation. Then, other researchers present techniques to determine temperature-dependent thermal properties (Aksöz *et al.*, 2010; Karimi *et al.*, 2010; Sadeghi *et al.*, 2011; Zamel *et al.*, 2012; Özturk *et al.*, 2013); however these techniques determine only one property. This work presents a method to estimate simultaneously temperature-dependent thermal conductivity, λ and volumetric heat capacity, ρc_p, of AISI 1045 steel.

Also, an uncertainty analysis is presented in this work as well a study of the contact resistance. The study on the contact resistance displays the influence of the Kapton layer on the resistive heater. The uncertainty analysis is done by taking into account the influence of the thermal contact resistance and the numerical and experimental temperature errors. In addition, the main purpose of the present work is to present the improvements performed in relation to Carollo *et al.* (2012).

2. THEORETICAL ASPECTS

2.1 Thermal Model

Figure 1 shows the proposed one-dimensional thermal model that consists of a sample located between a resistive heater and an insulator. To ensure the unidirectional heat flux, the sample much thinner than its other dimensions. In addition, all the surfaces, except the heated one (x = 0), were isolated (Fig. 2).

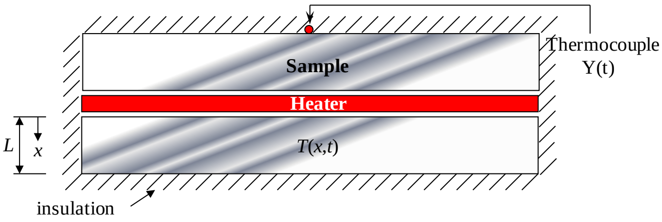

Figure 1. One-dimensional thermal model.

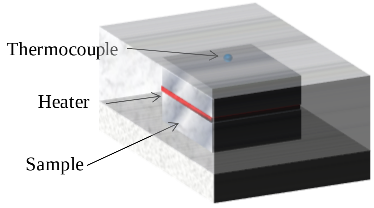

Figure 2. One-dimensional thermal model.

The heat diffusion equation for the problem presented in Figure 1 can be written as:

$$\frac{\partial}{\partial x}\lambda(T)\frac{\partial T(x,t)}{\partial x} = \rho c_p(T)\frac{\partial T(x,t)}{\partial t} \quad (1)$$

In accordance with the literature, there are two methods to estimate thermal properties dependent on temperature. In the first one, presented by Özisik (1993), the thermal model is based on nonlinear heat conduction, in others words, the properties are dependent on the temperature to solve the thermal model. The second method adopts constant thermal properties within a temperature range to solve the thermal model (Tillmann *et al.*, 2008). Thus, the initial temperature is defined (T_0) and the estimation of the properties occurs considering 5 ºC the maximum range of temperature. This condition is performed for all the desired temperature.

Therefore, the heat diffusion equation for the thermal problem with constant thermal properties can be written as:

$$\frac{\partial^2 T(x,t)}{\partial x^2} = \frac{\rho c_p}{\lambda}\frac{\partial T(x,t)}{\partial t} \quad (2)$$

subject to the boundary conditions:

$$-\lambda\frac{\partial T(x,t)}{\partial x} = \phi(t) \text{ at } x = 0 \quad (3)$$

$$\frac{\partial T(x,t)}{\partial x} = 0 \text{ at } x = L \quad (4)$$

and the initial condition:

$$T(x,t) = T_0 \text{ at } t = 0 \quad (5)$$

where x is the Cartesian coordinate, t the time, ϕ the prescribed heat flux, T_0 the initial temperature and L the thickness.

The numerical temperature is obtained through the solution of the one-dimensional diffusion equation using the Finite Difference method with an implicit formulation

2.2 Analyses of the best region to determine the properties ρc_p and λ

Studies of the sensitivity coefficient for each sample are performed in this work in order to determine the ideal region to estimate the properties and the best configuration of the experimental setup. This study provides information such as: the correct positioning of the thermocouples, the experimental time, and the time interval of the applied heat flux incidence. The higher the coefficient values, the better the chances of obtaining the properties reliably.

The sensitivity coefficient is defined by the first partial derivative of the temperature in relation to the parameter to be analyzed (ρc_p or λ), being written as follows:

$$X_{ij} = P_i\frac{\partial T_j}{\partial P_i} \quad (6)$$

where T is the numerical temperature, P is the parameter to be analyzed (ρc_p or λ), i is the index of parameter, and j is the index of points. As in this work, only two properties will be analyzed, i = 1 for ρc_p and i = 2 for λ.

Besides this, analyses of the objective function were performed in order to guarantee that in the analyzed region there is enough information to estimate the properties simultaneously. One can verify this information if a minimum value of the objective function is found when there are changes of the properties values. This function is represented by Eq. (7) in the next section.

2.3 Volumetric heat capacity and thermal conductivity simultaneous estimation

To estimate the two properties it is necessary to use an objective function based on the square difference between the experimental and numerical temperatures. This equation can be written as:

$$F = (R_c''\phi_m)^2 + \sum_{j=1}^{m}\left(Y_j - T_j\right)^2 \tag{7}$$

where, m is the total number of points, Y is the experimental temperature, R_c'' is the heater thermal contact resistance, and ϕ_m is the weighted average heat flux.

Thus, it is known that the optimal value for ρc_p and λ, that is, the value that minimizes the objective function is the value of the property to be estimated. To obtain this value, optimization techniques can be used, such as the BFGS (Broydon-Fletcher-Goldfarb-Shanno) sequential optimization technique used in this work and presented in Vanderplaats (2005). This technique is a particularity of Variable Metric Methods. The advantages of this method are the fast convergence and the ease to work with many design variables. Because it is a first order method, it is necessary to know the gradient of the objective function. This gradient is calculated numerically by using the computer package Design Optimization Tools - DOT (Vanderplaats, 2005).

3. EXPERIMENTAL PROCEDURE

Figure 3 shows the experimental apparatus used to determine the properties of AISI 1045 steel dependent on temperature. The dimensions of the grinding plates are 99.9 x 99.9 x 11.9 mm^3. The resistive kapton heater has a resistance of 23.2 Ω and dimensions of 99.5 x 99.5 x 0.2 mm^3. The resistive kapton heater was used for its thinness, allowing for faster overall warming. To provide the necessary heat flux, this heater was connected to a digital power supply Instrutemp ST – 305D-II. This experimental apparatus can be used from environment temperature up to 200 ºC.

In this work, different intensities of heat flux were used in the same experiment as an attempt to achieve the best condition for estimating the properties simultaneously in accordance with the analyses of the sensitivity coefficients. To achieve this heat flux condition, the digital power supply had a configuration that allowed work in parallel, series or independent connections. Thus, it is possible to apply different intensities of heat flux having the correct setup of the resistances which is by the combination of two buttons. Therefore, the following procedure was adopted: the series condition was used to provide the highest heat flux in the first period of the experiment, and, in the second part, the parallel condition to supply the lowest heat flux. A symmetrical assembly was used to minimize the errors when measuring the heat flux on the sample surface. In addition, the values of the current and resistance of the heater were measured with the calibrated multimeters Instrutherm MD-380 and Minipa ET-2042C, respectively.

To ensure a unidirectional heat flux and minimize the effect of convection caused by the air circulating in the environment, the heater-samples set was isolated with ceramic fiber plates. Temperatures were measured by using type T thermocouples (30AWG; 0.254 mm of diameter) welded by capacitive discharge in the middle of the bottom surface and calibrated by using Marconi MA 184 bath temperature calibrator with a resolution of ± 0.01 K. This thermocouple was connected to an Agilent 34980A data acquisition, controlled by a microcomputer. The assembly was located inside a Marconi MA030 oven to control the desired initial temperature. To obtain better results, all experiments were performed in a temperature controlled room.

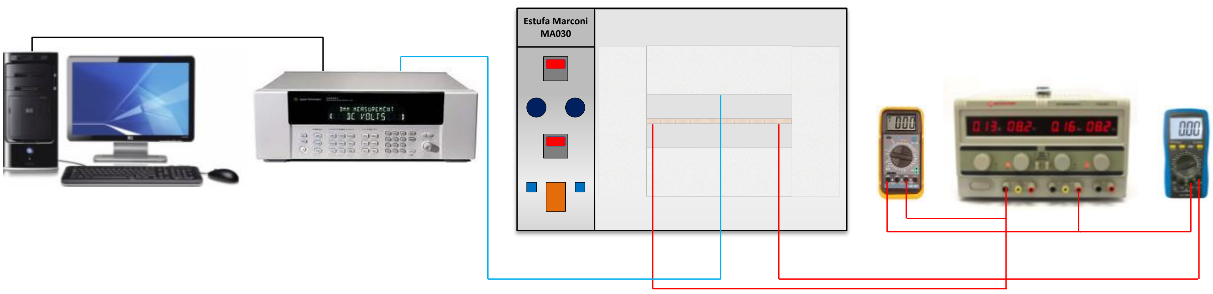

Figure 3. Sketch of the experimental apparatus used to determine the properties.

4. RESULTS ANALYSES

Fifteen experiments were performed to simultaneously estimate the thermal conductivity and the volumetric heat capacity of AISI 1045 steel for each initial temperature (25ºC, 50ºC, 75ºC, 100ºC, 125ºC e 150ºC). Each experiment lasted 80 s, but the heat flux was imposed from 0 to 70 s. In the first part, from 0 to 10 s, the imposed heat flux was approximately 7709 Wm^{-2}. For the second part, from 10 to 70 s, the imposed heat flux was around 1854 Wm^{-2}. The time interval used to monitor the temperature was 0.1 s. To guarantee the hypotheses of constant thermal properties, this configuration for the heat fluxes was chosen to keep the temperature difference lower than 5 K. This temperature difference is based on the difference between the final and initial temperatures which are measured on the same position of the sample.

The sensitivity analyses were performed to determine the best region to estimate the properties. These analyses were performed using the values of λ and ρc_p obtained from Incropera *et al*. (2011) and the parameters described above. In addition, several analyses of the objective function (Eq. 7) with the sensitivity coefficient analyses were performed to determine the properties in the selected region. This selected region corresponds to a set of points which provide accurate thermal property estimation. Since this estimation presents an accurate result, it can be said that this region of points presents enough influence to determine these properties.

Figure 4 shows the sensitivity coefficients at $x = L$ for λ and ρc_p, and Fig. 5 presents the values of the objective function.

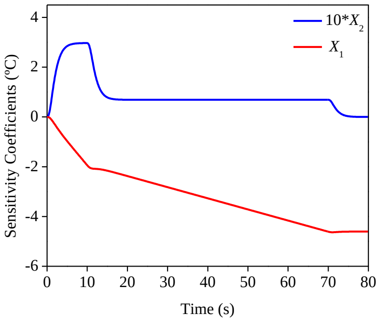

Figure 4. Sensitivity Coefficients.

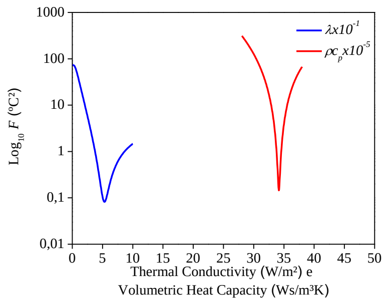

Figure 5. Objective Function Values (F).

X_2 represents the sensitivity coefficient for λ and X_1 represents the sensitivity coefficient for ρc_p, both on the isolated surface. The former is multiplied by a factor to provide a better view of the curve. In Figure 4, one can see that X_2 increases during the first 9 seconds and remains constant thereafter until the change of heat flux; and X_1 increases proportionally with the temperature.

Because of this behavior, a higher heat flux was imposed in the first period of time, resulting in high sensitivity for λ. A lower heat flux was imposed in the second part to increase the sensitivity for ρc_p and maintain the sensitivity for λ. This procedure was done, because it is necessary to control the magnitude relation between X_1 and X_2, to guarantee that both properties are estimated. That is, if one coefficient is much larger than the other, the estimation, by using minimization, will occur only for that property that presents the higher coefficient. Hence, Figure 5 shows that, since a minimum value was found for each property, enough influence exists to simultaneously determine the properties in the region analyzed. Figure 5 was obtained by minimizing the difference between the experimental and numerical temperatures. This numerical temperature was obtained by varying the value of one property while the other property was kept constant. Thus, the minimum value, in other words, the estimated property, was found when the temperature difference presented the lowest value for all the property values analyzed. On analyzing Fig. 5, it can be seen that there is a different minimum value for each property; however the estimation occurs at the same time for the properties by using the same objective function.

Another objective of the sensitivity analysis is to determine the number of points in the curve which should be used to estimate the properties. To be considered in properties estimation, these points should have derivatives different from zero, which indicates applied heat flux. So, the sets of points which do not present applied heat flux should be disregarded in the estimation. Also, a thermal inertia analysis of the heater was carried out to verify whether this inertia can cause an influence in the experiments. This analysis was performed by using an assembly which contained heat flux sensors, similar to Borges *et al*. (2006). Therefore, it was possible to quantify this thermal inertia in time. These tests were done by applying the same experimental conditions and the results presented a delay of almost 2 seconds to achieve the real value of heat flux. Thus, the set of points which corresponded to this delay was disregarded in the thermal properties estimation.

To determine whether the conditions explained above resulted in good experiments, another analysis was performed based on Dowding *et al*. (1995). According to these authors, the best condition and design for the experiment were achieved when the sum of the sensitivity coefficient to λ and ρc_p plus the temperature difference were equal to zero ($X_1 + X_2 + Y - Y_0 = 0$). For this, the boundary conditions of imposed heat flux on the top surface and insulation on the bottom surface were considered. In other words, if this proposed condition is reached, the reliability of the obtained results can be guaranteed. Figure 6 shows the obtained results of this analysis considering the above experiment.

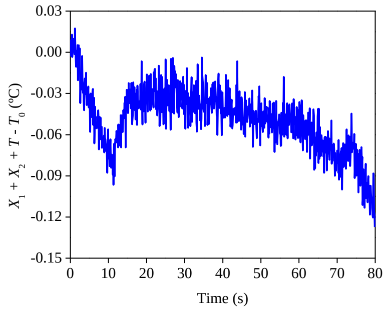

Figure 6. Analysis for the best condition and design for 1045 steel.

One can see that the result for this analysis is satisfactory, because the highest difference was around 0.12 ºC. Thus, this proves that experiment was well performed.

To improve the analyses of this work, the thermal contact resistance was analyzed with the purpose to find out if there is a significant influence during the temperature measurements. In this study, the influence of the kapton layer present in the resistance heater was taken into account. Two factors were considered for this analysis: the thermal conductivity and the thickness of the heater kapton layer. An Optical Microscope Jenavert Zeiss (2000x) with the Image Analyzer Olympus Model TVO.5XC-3 was used to measure the thickness of the kapton on the heater. The kapton layer presents a thickness of $10.64\text{x}10^{-6}$ m. As the thermal conductivity of the kapton is 0.12 $\text{Wm}^{-1\text{o}}\text{C}^{-1}$ (MatWeb, 2015), a thermal contact resistance is equal to $88.67\text{x}10^{-6}$ $\text{m}^{2\text{o}}\text{CW}^{-1}$. By considering the applied weighted average heat flux of 2639.95 Wm^{-2}, this thermal contact resistance corresponds to a temperature difference of 0.23 ºC.

Figure 7 presents the distribution for experimental and numerical temperatures on the plate, at $x = L$ and the imposed heat flux at $x = 0$. The numerical temperature is achieved by employing the property values of ρc_p and λ estimated for one of the accomplished experiments. These temperatures present good concordance which can be proved by analysis of the temperature residuals. The temperature residuals are shown in Figure 8, in other words, it is the difference between the experimental and the numerical temperatures. One observes the good agreement of the results for the AISI 1045 steel. For the thermocouple located on the opposite surface, a difference of up to 0.10 ºC was sensed. These deviations may be due to the contact resistance between the resistive heater and the sample, and the difficulty of isolating the experiment.

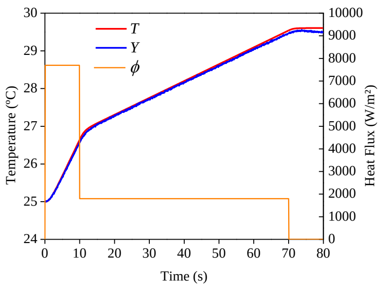

Figure 7. Numerical (T) and Experimental (Y) Temperatures with Heat Flux (ϕ) for AISI 1045 steel.

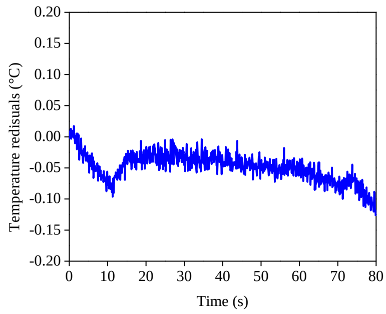

Figure 8. Temperature residuals for 1045 steel.

Table 1 presents the mean value, the standard deviation and the error (the percentage difference between the mean and the literature value) for ρc_p and λ of AISI 1045 steel with the oven temperature set at 25 ºC.

Table 1. Results obtained for the AISI 1045 steel with the oven temperature set at 25 ºC.

Average T_0 (ºC)	**Property**	**Mean**	**Grzesik *et al.* (2009)**	**S. D.**	**Error (%)**
25.4	**$\rho c_p \text{x}10^{-6}$ (Ws/m³K)**	3.48	3.43	± 0.02	1.44
	λ (W/mK)	52.04	51.80	± 0.49	0.46

The estimated values of ρc_p and λ, when compared with the literature values, are in good agreement. Moreover, the error found in estimating the thermal conductivity is consistent when compared with the values found in literature.

Thus, the technique proposed is validated and the experiments can be carried out for the other initial temperatures. Only the results will be presented, because the analyses were performed by following the same procedure.

Tables 2 to 6 present the mean value, the standard deviation and the error (the percentage difference between the mean and the literature value) for ρc_p and λ of AISI 1045 steel for each initial temperature.

Table 2. Results obtained for the AISI 1045 steel with the oven temperature set at 50 ºC.

Average T_0 (ºC)	**Property**	**Mean**	**Grzesik *et al*. (2009)**	**S. D.**	**Error (%)**
46.1	ρc_p**x10^{-6} (Ws/m³K)**	3.54	3.50	± 0.52	1.18
	λ **(W/mK)**	51.39	51.4	± 0.25	0.02

Table 3. Results obtained for the AISI 1045 steel with the oven temperature set at 75 ºC.

Average T_0 (ºC)	**Property**	**Mean**	**Grzesik *et al*. (2009)**	**S. D.**	**Error (%)**
69.4	ρc_p**x10^{-6} (Ws/m³K)**	3.59	3.54	± 0.04	1.36
	λ **(W/mK)**	50.92	51.00	± 0.37	0.16

Table 4. Results obtained for the AISI 1045 steel with the oven temperature set at 100 ºC.

Average T_0 (ºC)	**Property**	**Mean**	**Grzesik *et al*. (2009)**	**S. D.**	**Error (%)**
92.4	ρc_p**x10^{-6} (Ws/m³K)**	3.61	3.66	± 0.03	0.99
	λ **(W/mK)**	50.47	50.40	± 0.28	0.14

Table 5. Results obtained for the AISI 1045 steel with the oven temperature set at 125 ºC.

Average T_0 (ºC)	**Property**	**Mean**	**Grzesik *et al*. (2009)**	**S. D.**	**Error (%)**
115.3	ρc_p**x10^{-6} (Ws/m³K)**	3.66	3.61	± 0.05	1.42
	λ **(W/mK)**	49.75	49.80	± 0.38	0.10

Table 6. Results obtained for the AISI 1045 steel with the oven temperature set at 150 ºC.

Average T_0 (ºC)	**Property**	**Mean**	**Grzesik *et al*. (2009)**	**S. D.**	**Error (%)**
139.2	ρc_p**x10^{-6} (Ws/m³K)**	3.74	3.77	± 0.02	0.86
	λ **(W/mK)**	49.55	49.40	± 0.36	0.30

On analyzing the standard deviation, one can see that the results present better precision for ρc_p, due to its greater sensitivity coefficient than λ. Besides, the maximum difference between the literature and the experimental results was 2 %, which guarantees the good quality of the experiments.

Figures 9 and 10 present the literature and experimental result values. One can see the good agreement of the curves, which present a correlation factor of 0.98.

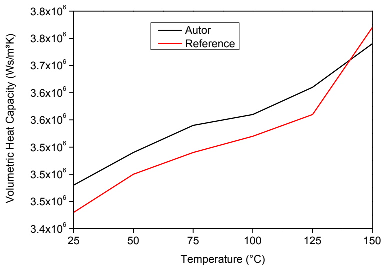

Figure 9. Comparison of the literature with the obtained results for ρc_p.

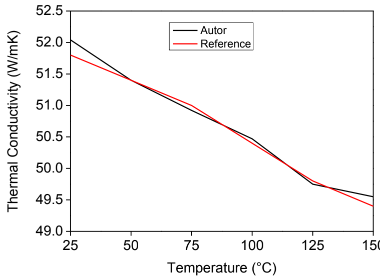

Figure 10. Comparison of the literature with the obtained results for λ.

From these results, the equations for the volumetric heat capacity and thermal conductivity can be written as:

$$\lambda(T) = -0.02228\,T + 52.500 \tag{8}$$

$$\rho c_p(T) = (0.00210\,T + 3.43253)10^6 \tag{9}$$

5. UNCERTAINTY ANALYSIS

An uncertainty analysis was done to verify whether the results obtained were reliable. This analysis was based on the uncertainty propagation procedure. In this procedure, it is necessary to decide which errors will be analyzed. Thus, the following errors were considered: temperature measurement, the imposed heat flux, measurement instruments, thermal contact resistance, imperfection of thermal insulation, and the numerical errors (BFGS and Finite Difference method-FDM). Therefore, the uncertainty analysis can be done by the sum of these considered errors in accordance with the theory of error propagation extracted from Taylor (1997).

When analyzing the experimental temperature for the AISI 1045 steel, the thermocouple error, the thermal contact resistance, the acquisition data error, and the imperfection of thermal insulation were considered. Thus:

$$U_Y^2 = U_{aquis}^2 + U_{therm}^2 + U_{contactresis}^2 + U_{insul}^2 \tag{10}$$

The errors of the multimeters used to measure the current and the heater resistance values as well as the numerical error of the Finite Difference method were used to calculate the uncertainty numerical temperature. Therefore:

$$U_T^2 = U_{current}^2 + U_{resistance}^2 + U_{MDF}^2 \tag{11}$$

Finally, the uncertainty of the estimation can be calculated based on the objective function, which is composed of the experimental and numerical temperatures and the BFGS method. Hence:

$$\begin{aligned} U_{final}^2 &= U_Y^2 + U_T^2 + U_{BFGS}^2 \\ U_{final}^2 &= U_{aquis}^2 + U_{therm}^2 + U_{contactresis}^2 + U_{insul}^2 + U_{current}^2 + U_{resistance}^2 + U_{MDF}^2 + U_{BFGS}^2 \end{aligned} \tag{12}$$

After the final uncertainty has been defined, it is necessary to quantify the partial uncertainty. To define these values, the authors decided to consider each uncertainty divided by the mean value of the analyzed parameter, except for the temperature, which considered the maximum difference between the initial and final temperature in the same experiment. Thus, uncertainties are:

$$U_{aquisition\,data} = \frac{0.01}{5} = 0.20\ \% \qquad U_{thermocouple} = \frac{0.10}{5} = 2.00\ \%$$

$$U_{contact\ resistance} = \frac{0.23}{5} = 4.60\ \% \qquad U_{thermal\ \ insulation} = \frac{0.10}{5} = 2.00\ \%$$

$$U_{current\,multimeter} = \frac{0.01}{1.98} = 0.51\ \% \qquad U_{resistance\ multimeter} = \frac{0.10}{24.4} = 0.41\%$$

$$U_{BFGS} = \frac{0.01}{5} = 0.20\ \% \qquad U_{MDF} = \frac{0.01}{5} = 0.20\ \%$$

Thus, the final uncertainty:

$$\begin{aligned} U_{final}^2 &= 0{,}20^2 + 2{,}00^2 + 4{,}60^2 + 2{,}00^2 + 0{,}51^2 + 0{,}41^2 + 0{,}20^2 + 0{,}20^2 \\ U_{final}^2 &= 5{,}45\% \end{aligned} \tag{13}$$

As it can be seen, the uncertainty value is in accordance with that found in literature, because the presented value is around 5 %.

6. CONCLUSIONS

This paper presents a technique for the simultaneous estimation of temperature-dependent volumetric heat capacity and thermal conductivity of metallic materials by applying different intensities of heat flux. The material analyzed was the AISI 1045 steel. Good results were found. This affirmation can be proved due to the small difference between the literature and estimated values, and the low standard deviation. For future work, the use of a three-dimensional thermal model is proposed to analyze the placement of thermocouples in various points of the sample, so as to find regions which present higher sensitivity to determine these properties.

7. ACKNOWLEDGEMENTS

The authors would like to thank CNPq, FAPEMIG and CAPES for their financial support.

8. REFERENCES

Aksöz, S., Ocak, Y., Marasli, N., Cadirli, E., Kaya, H., Böyük, U., 2010, “Dependency of the Thermal and Electrical Conductivity on the Temperature and Composition of Cu in the Al based Al–Cu Alloys”, Experimental Thermal and Fluid Sciences, Vol. 34, pp. 1507-1516.

Borges, V.L., Lima e Silva, S.M.M., Guimarâes, G., 2006, “A Dynamic Thermal Identification Method Applied to Conductor and Non Conductor Materials”, Inverse Problems in Science and Engineering, Vol. 14, pp. 511-527.

Brito, R.F., Carvalho, S.R., Lima E Silva, S.M.M., 2015 “Investigation of Thermal Aspects in a Cutting Tool Using Comsol and Inverse Problem”, Applied Thermal Engineering, Vol. 86, pp. 60-68.

Carollo, L.F.S., Lima e Silva, A.L.F., Lima e Silva, S.M.M., 2012, “Applying Different Heat Flux Intensities to Simultaneously Estimate the Thermal Properties of Metallic Materials”, Measurement Sciences and Technology, Vol. 23, pp. 1-10.

Dowding, K.J., Beck J., Ulbrich, A., Blackwell, B., Hayes J., 1995, “Estimation of Thermal Properties and Surface Heat Flux in Carbon-Carbon Composite”, Journal of Thermophysics and Heat Transfer, Vol. 9, pp. 345-351.

Grzesik, W., Nieslony, P., Bartoszuk, M., 2009, “Modelling of the Cutting Process Analytical and Simulation Methods”, Advances in Manufacturing Sciences and Technology, Vol. 33, pp. 6-29.

Incropera, F.P., Dewitt, D.P., Bergman, T.L., Lavine, A.S., 2011, Fundamentals of Heat and Mass Transfer, John Wiley & Sons, 7th ed., USA, 1072p.

Jannot, Y.,Degiovanni, A.,Payet, G., 2009, “Thermal conductivity measurement of insulating materials with a three layers device”, International Journal of Heat and Mass Transfer, Vol. 52, pp. 1105-1111.

Karimi, G., Li, X., Teerstra, P., 2010, “Measurement of Through-plane Effective Thermal Conductivity and Contact Resistance in PEM Fuel Cell Diffusion Media”, Electrochimica Acta, Vol. 55, pp. 1619-1625.

Matweb, 2015, “Kapton - Polyamide layer”, Matweb – Material Property Data. 22 Feb. 2015 < http://www.matweb.com/search/DataSheet.aspx?MatGUID=99c680bc28dd409fb7e8fd3ddbcee537>

Özisik, M.N., 1993, Heat Conduction, John Wiley & Sons, 2th ed., Canada, 692p.

Öztürk, E., Aksöz, S., Keslioglu, K., Marasli, N., 2013, “The Measurement of Thermal Conductivity variation with Temperature for Sn-20 wt.% In based Lead-free Ternary Solders”, Thermochimica Acta, Vol. 554, pp. 63-70.

Sadeghi, E., Djilali, N., Bahrami, M.,2011, “A Novel Approach to Determine the In-plane Thermal Conductivity of Gas Diffusion Layers in Proton Exchange Membrane Fuel Cells”, Journal of Power Sources, Vol. 196, pp. 3565-3571.

Santos, M.R., Lima E Silva, S.M.M., Machado, A.R., Silva, M.B., Guimarães, G., Carvalho, S.R., 2014, “Analyses of Effects of Cutting Parameters on Cutting Edge Temperature Using Inverse Heat Conduction Technique, Mathematical Problems in Engineering, Vol. 2014, pp. 1-11.

Taylor, J.R., 1997, An introduction to error analysis: the study of uncertainties in physical measurements, University Science Books, 2nd ed.,USA, 488p.

Thomas, M., Boyard, N., Lefèvre, N., Jarny, Y.,Delaunay, D., 2010, “An experimental device for the simultaneous estimation of the thermal conductivity 3-D tensor and the specific heat of orthotropic composite materials”, International Journal of Heat and Mass Transfer, Vol. 53, pp. 5487-5498.

Tillmann, A.R., Borges, V.L., Guimarães, G., Lima e Silva, A.L.F., Lima e Silva, S.M.M., 2008, “Identification of Temperature-Dependent Thermal Properties of Solid Materials”, Journal of the Brazilian Society of Mechanical Science and Engineering, Vol. 30, pp. 269-278.

Vanderplaats, G.N., 2005, Numerical Optimization Techniques for Engineering Design, McGraw, 4th ed., USA, 465p.

Xamán, J., Lira, L., Arce, J., 2009, “Analysis of the temperature distribution in a guarded hot plate apparatus for measuring thermal conductivity”, Applied Thermal Engineering, Vol 29, pp. 617-623.

Zamel, N., Becker, J. Wiegmann, A., 2012, “Estimating the Thermal Conductivity and Diffusion Coefficient of the Microporous Layer of Polymer Electrolyte Membrane Fuel Cells”, Journal of Power Sources, Vol. 207, pp. 70-80.

9. RESPONSIBILITY NOTICE